

Dimensionality-enhanced quantum state transfer in long-range interacting spin systems

Samihr Hermes,^{1,*} Tony J. G. Apollaro,² Simone Paganelli,^{3,†} and Tommaso Macrì^{1,4,3,‡}

¹*Departamento de Física Teórica e Experimental,
Universidade Federal do Rio Grande do Norte, Natal-RN, Brazil*

²*Department of Physics, University of Malta, Msida MSD 2080, Malta[§]*

³*Dipartimento di Scienze Fisiche e Chimiche, Università dell'Aquila, via Vetoio, I-67010 Coppito-L'Aquila, Italy*

⁴*International Institute of Physics, Natal-RN, Brazil*

(Dated: December 16, 2019)

In this work we study the single-qubit quantum state transfer in uniform long-range spin XXZ systems in high-dimensional geometries. We consider prototypical long-range spin exchanges that are relevant for experiments in cold atomic platforms: Coulomb, dipolar and van der Waals-like interactions. We find that in all these cases the fidelity increases with the dimensionality of the lattice. This can be related to the emergence of a pair of bilocalized states on the sender and receiver site due to the onset of an effective weak-coupling Hamiltonian. The enhancement of the quantum state transfer fidelity is more pronounced both with the increase of the couplings interaction range and in going from a 1D to a 2D lattice. Finally, we test our predictions in the presence of temperature-induced disorder introducing a model for the thermal displacement of the lattice sites, considered as a set of local adiabatic oscillators.

I. INTRODUCTION

Quantum information processing requires suitable transfer protocols for transmitting a quantum state between different parties. This task results to be nontrivial because of the decoherence induced by the unavoidable interaction with an environment. Quantum State Transfer (QST) has been achieved over large distances by spatial transmission of the particle carrying the state (*flying qubit*) [1–4]. Photons are a natural choice for flying qubits and this strategy has been successfully employed in cavity QED devices. Another option, also suitable for long-distance transmission, is creating an entangled state to be shared between the parties, sender and receiver, in order to implement a teleportation protocol[5, 6].

However, photons are not always the ideal choice to implement scalable quantum architectures where an efficient short-distance transmission is requested, e.g., in solid state based quantum computers. Here a more desirable option would be exploiting the natural dynamics of some excitations carrying the quantum information encoded in its quantum state. The most widely investigated model to perform such a task results to be a spin- $\frac{1}{2}$ Hamiltonian, where the initial state is encoded into one or more spins, accessible to a sender, and it is retrieved, after a certain time, on an equivalent set of spins accessible to a receiver [7–10].

Different strategies have been proposed to optimize the QST fidelity: almost perfect state transfer can be obtained in time-independent uniform chains [11–13], by modulated interactions [8, 14], in disordered

chains [15, 16], exploiting the ballistic regime of the excitations [8, 17–21], in the regime of weakly coupled sender/receiver [11, 12, 20, 22–25], creating nearly-resonant edge states introducing strong magnetic fields [23, 26, 27], and by topological protection [28, 29] (For more detailed reviews see [30, 31]).

Many steps forward have been done, both concerning the QST of many qubit system [32–34], and in the implementation schemes ranging from optomechanical arrays [35], quantum dots [36–39] to ultracold atoms [24, 40].

A lot of effort has been put into accomplishing quantum computing hardware with atom traps [41–43], since these schemes can be easily mapped into a many-body spin-1/2 model. In this context, different systems, such as polar molecules, trapped ions, Rydberg atoms, are characterized by long-range interactions, possibly mediated by long-wavelength modes such as cavity photons, decreasing with distance as a power law. Here some of the results obtained for next nearest neighbors interactions do not apply, in particular the estimation of the transmission time becomes more demanding because of the breakdown of the Lieb-Robinson bound [44]. QST has been studied for long-range interacting systems [16, 45–48] with high fidelity and time speedup.

In this paper we analyze different long-range spin models and we show that when the quantum channel is made of a two-(three-)dimensional lattice with uniform coupling, it is possible to achieve larger fidelity with respect to the case of a one-dimensional channel with the same Hamiltonian parameters.

In Sec.(II) we define the spin model and review the basic features of QST in quantum spin chains with short and long-range couplings. In Sec.(III) we discuss our results on QST with paradigmatic long-range spin exchange scaling as $1/r^\alpha$ ($\alpha > 0$) as the Coulomb interaction ($\alpha = 1$), dipolar ($\alpha = 3$) and van der Waals ($\alpha = 6$), as well as the case of ($\alpha = 1/2$) relevant for ion-trap ex-

* hermes@fisica.ufrn.br

† simone.paganelli@univaq.it

‡ macri@fisica.ufrn.br

§ tony.apollaro@um.edu.mt

periments in one, two and three dimensional geometries. In Sec. (III A) we analyze the effect of vacancies as a way to improve the QST in these models and interpret the results by looking at the spectrum of effective two-spin models. The relevance of symmetry in the removal of spins in the chain is emphasized. In Sec.(III B) we discuss finite temperature effects leading to a displacement of the spins with respect to their equilibrium position. Finally, in Sec.(IV) we present our conclusions and propose some extensions of our work.

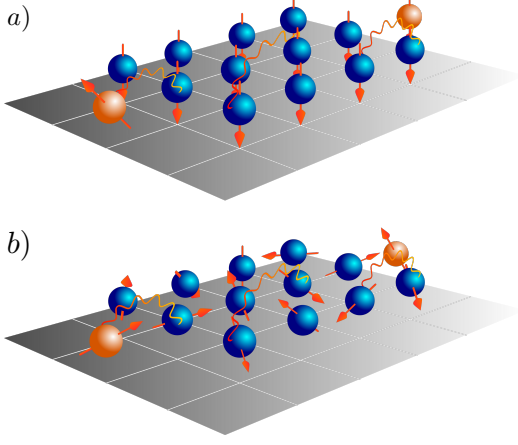


FIG. 1. Dynamical evolution of a quantum spin system with long-range interactions in a two-dimensional array. Sender and receiver (orange) and the channel (blue) interact via a long-range spin-exchange interaction $1/r^\alpha$. At $t = 0$ the system is the state $|\psi_s\rangle = \alpha|0\rangle + \beta|1\rangle$ with one excitation localized at the sender $i = 1$. After a certain time t the state $|\psi_s\rangle$ of the sender can be found with high fidelity at the receiver $i = N$.

II. QUANTUM STATE TRANSFER IN THE XXZ MODEL.

We consider a long-range XXZ spin model with Hamiltonian

$$\hat{H} = \sum_{\substack{i,j=1 \\ i < j}}^N \frac{C}{2a^\alpha |\mathbf{r}_i - \mathbf{r}_j|^\alpha} \left(\hat{S}_i^+ \hat{S}_j^- + \hat{S}_i^- \hat{S}_j^+ + 2\Delta \hat{S}_i^z \hat{S}_j^z \right), \quad (1)$$

where S^\pm and S^z are spin-1/2 operators. The couplings C and Δ denote the intensity of the spin-exchange interaction and the anisotropy parameter, whereas α is the power-law exponent the long-range coupling. Finally a is the lattice spacing among nearest neighbor spins in the lattice. For simplicity we set $C = 1$ in units of Energy $\times a^\alpha$ throughout our work, while \mathbf{r}_i are dimensionless positions of the spins in units of a . For $\Delta = 0$ one obtains the isotropic long-range XY model, for $\Delta = 1$ one recovers the isotropic long-range Heisenberg model, and for $\Delta = \infty$ we obtain the long-range (classical) Ising

model. The nearest-neighbor ($\alpha = \infty$) isotropic Heisenberg model was first considered in the seminal paper by Bose in [?]. See Appendix A for the generalization of these results to higher dimensions. In this work we vary the long-range exponent $\alpha > 0$ and set the anisotropy parameter $\Delta = -2$. We notice that for $\Delta = -2$ we can rewrite the spin couplings in the form of a dipolar exchange potential

$$\hat{H}_{dip} = \sum_{ij} J_{ij} \left(\hat{\mathbf{S}}_i \cdot \hat{\mathbf{S}}_j - 3\hat{S}_i^z \hat{S}_j^z \right), \quad (2)$$

where $J_{ij} = C/2a^\alpha |\mathbf{r}_i - \mathbf{r}_j|^\alpha$.

The protocol describing the dynamics of our setup is described in Fig.1 for a two-dimensional setup. The one- and three-dimensional setups will be explicitly discussed below. In fig.(1)a the system of N spin-1/2 is initialized in the ferromagnetic state $\otimes_i |\downarrow\rangle_i$ in the z -basis. At $t = 0$ one spin, the sender (in orange) is placed into a state $|\psi_s\rangle = \cos \frac{\theta}{2} |\downarrow\rangle + e^{i\phi} \sin \frac{\theta}{2} |\uparrow\rangle$. Here $\theta \in [0, \pi]$ and $\phi \in [0, 2\pi]$ are the usual angles defining a single qubit state in the Bloch sphere. The system is then left to evolve under unitary dynamics with the Hamiltonian eq.(1). Additional effects such as decoherence, excited state decay, or a generic coupling to an external reservoir, will be considered elsewhere, while the effects of temperature-induced positional disorder will be thoroughly discussed in Sec. III B.

We observe that for the model we are considering the total magnetization is preserved, i.e., $[\hat{H}, \sum_{i=1}^N S^z] = 0$. Therefore the Hilbert space where the dynamics takes place is confined to the zero-excitation sector consisting of the fully ferromagnetic state $\otimes_i |\downarrow\rangle_i$ and the one excitation sector consisting of N states, where $N - 1$ spins are in the $|\downarrow\rangle$ configuration and one is in the $|\uparrow\rangle$ configuration. Under these conditions one can redefine the many-body states in the computational basis as

$$\otimes_i |\downarrow\rangle_i \equiv |\mathbf{0}\rangle; \quad (3)$$

$$|\uparrow\rangle_j \otimes_{i \neq j} |\downarrow\rangle_i \equiv |\mathbf{j}\rangle, \quad (4)$$

that belong to a subspace \mathbf{H} of dimension $N + 1$ of the full Hilbert space. For our calculations we perform exact numerical diagonalization of the Hamiltonian matrix of eq.(1) in the basis above. Taking $\frac{C}{2a^\alpha} = 1$, we have the diagonal and off-diagonal elements

$$\langle \mathbf{j} | H | \mathbf{j} \rangle = \frac{\Delta}{2} \left(\sum_{\substack{k,l=1 \\ k \neq l}}^N \frac{1}{|\mathbf{r}_k - \mathbf{r}_l|^\alpha} - \sum_{\substack{i=1 \\ i \neq j}}^N \frac{1}{|\mathbf{r}_i - \mathbf{r}_j|^\alpha} \right), \quad (5)$$

$$\langle \mathbf{i} | H | \mathbf{j} \rangle = \frac{1}{|\mathbf{r}_i - \mathbf{r}_j|^\alpha}. \quad (6)$$

For the special case of nearest neighbor exchange inter-

actions one has

$$\langle \mathbf{i} | H | \mathbf{j} \rangle = \begin{cases} 0 & \text{if } |\mathbf{r}_i - \mathbf{r}_j| \neq 1; \\ 1 & \text{otherwise.} \end{cases}$$

$$\langle \mathbf{j} | H | \mathbf{j} \rangle = \sum_{\substack{i,k=1 \\ i < k}}^N S_{ik}.$$

where

$$S_{ik} = \begin{cases} \frac{\Delta}{2} & \text{if } |\mathbf{r}_i - \mathbf{r}_k| = 1 \text{ and } j \neq i, k; \\ -\frac{\Delta}{2} & \text{if } |\mathbf{r}_i - \mathbf{r}_k| = 1 \text{ and } j = i \text{ or } j = k; \\ 0 & \text{otherwise.} \end{cases} \quad (7)$$

As a figure of merit of the quality of the QST from the sender to the receiver (orange spins in fig.(1)) we use the fidelity

$$F(t) = \int \frac{d\Omega}{4\pi} \langle \psi_s(t) | \rho_r(t) | \psi_s(t) \rangle \quad (8)$$

where $\rho_r(t)$ is the density matrix of the spin at the receiver site N and the average is taken over the initial state of the sender.

Upon integration we obtain the general expression

$$F(t) = \frac{1}{6} |f_{r,s}(t)|^2 + \frac{1}{3} |f_{r,s}(t)| + \frac{1}{2}. \quad (9)$$

where we defined $f_{r,s}(t) = |\langle \mathbf{r} | e^{-i\hat{H}t} | \mathbf{s} \rangle|$ and set $\hbar = 1$. $|\mathbf{s}\rangle$ and $|\mathbf{r}\rangle$ are the singly-excited states localized at the sender and receiver respectively. In the calculation of $F(t)$ we also neglected the term $\cos(\gamma)$, where γ is the phase of the amplitude $\langle \mathbf{r} | e^{-i\hat{H}t} | \mathbf{s} \rangle$.

In the next paragraphs we analyze the dynamics of $F(t)$ for configurations in one, two and three dimensions as a function of the power-law exponent α .

III. QUANTUM STATE TRANSFER WITH LONG-RANGE COUPLINGS.

In this Section we discuss the maximum fidelity achievable for the QST in a long-range interacting system in one, two and three dimensions for different power-law interaction potentials. In fig.(2) we show the results of the simulations. In the one dimensional configuration (red dots) sender and receiver are located at the extremes of the chain. In 2D (blue squares) we consider a rectangle lattice with $N \times 5$ spins where sender and receiver are placed as in fig.(1). In 3D (grey diamonds) we examine a cubic lattice with $(N \times 5 \times 5)$ spins where sender and receiver are located in the center of two opposite faces of the parallelepiped with 5×5 spins, at the distance a from the central spin. The exponent of the power-law interaction that we analyze are a) $\alpha = 0.5$, b) $\alpha = 1$, c) $\alpha = 3$, and d) $\alpha = 6$. We notice that the higher the dimensionality of the lattice and the range of the interaction, the

higher is the fidelity. Furthermore, the enhancement is more pronounced the larger the system and, in 3D lattices, the fidelity even stays close to one for relatively large system sizes.

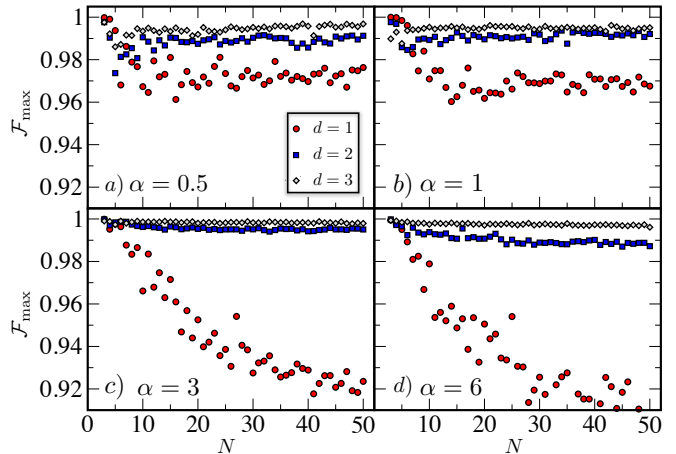


FIG. 2. Maximum fidelity for quantum state transfer in a long-range interacting system in one, two and three dimensions for different power-law interaction potentials and $\Delta = -2$. Red dot: $d = 1$, blue square: $d = 2$, grey diamond: $d = 3$. N is the linear size of the system. In 2D (3D) we consider a rectangle (parallelepiped) lattice with $N \times 5$ ($N \times 5 \times 5$) spins. In 2D the sender and the receiver are located as in Fig.1. In 3D they are located in the center of the square-section of opposite faces of the parallelepiped, at the distance a from the central spin. The exponent of the power-law interaction is a) $\alpha = 0.5$, b) $\alpha = 1$, c) $\alpha = 3$ and d) $\alpha = 6$. Fidelity increases with the dimensionality of the system for each power-law interaction. We notice that in 3D the fidelity stays close to one even for a large system size.

The dimensionality and interaction-range enhanced fidelity can be traced back to the onset of an effective weak-coupling regime taking place because of the open boundary conditions of the lattice at whose edges the sender and receiver spin are coupled symmetrically. Protocols exploiting the weak-coupling regime between sender (receiver) and a quantum channel for QST have been widely explored mainly in one-dimensional lattices. In 1D and in the presence of short-range Hamiltonian, to obtain the Rabi-like oscillations of the excitation between the sender and the receiver site, it is necessary effectively decouple the sender and the receiver site from the quantum wire. This can be obtained both by acting on the respective hopping term and on the on-site magnetic field in the Hamiltonian, or on both at the same time. Here we consider a Hamiltonian with uniform coupling and the onset of an effective weak-couplings regime is a combined effect of the lattice dimensionality, the range of the interaction and the presence of the spin-exchange interaction term in the transverse z direction. The effect of the latter on the Hamiltonian in the single-excitation sector mimics that of an effective non-homogeneous on-site magnetic field in the z -direction with values given by Eq. 5.

To explain in a quantitative way the increase of the

maximum of the fidelity with the dimensionality, we analyze the eigenvectors of the Hamiltonian in eq.(1) that have maximum overlap with the sender and the receiver. We observe that for the topology we discuss in this work by increasing the dimensionality of the lattice, the connectivity of the sender and the receiver with the neighbor spins of the channel (with strongest coupling) decreases with respect to the connectivity of the channel spins in the bulk. The ratio of the connectivities of the sender/receiver with the channel spins equals $C_{s/r}/C_c = 1/2, 1/4, 1/6$ respectively in one, two, and three dimensions. Therefore, the eigenstates localize more on the sender and receiver spin in higher dimensions, leading to a higher fidelity of the quantum state transfer.

A. Quantum state transfer in the presence of defects and the role of symmetry.

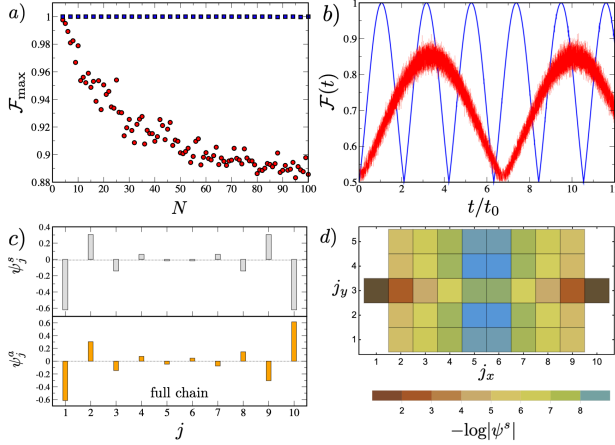


FIG. 3. Quantum state transfer for a long-range interacting one- and two-dimensional system with $\alpha = 6$ (van der Waals interactions) and $\Delta = -2$. a) Maximum value of the fidelity for a system with N spins ($N = 2, \dots, 100$). Red dots: One-dimensional chain with N spins. Blue squares: Two-dimensional $N \times 5$ setup as in d). b) Dynamical evolution of the fidelity as a function of the rescaled time t/t_0 . The time $t_0 = \pi a^\alpha (N-1)^\alpha / C \hbar^2$ is the time it takes for the two-spin system (sender and receiver) to perform an ideal quantum state transfer for $N = 50$. c) Symmetric and antisymmetric eigenstates $\psi_j^{(s,a)}$ with the greatest overlap with the sender and the receiver, which are responsible for the high-fidelity state transfer for the one-dimensional case. d) Overlap with highest overlap with the sender and the receiver for a two-dimensional system with 10×5 spins. Darker colors correspond to higher overlap.

In fig.(3)a we plot the maximum value of the fidelity for a system with N spins ($N = 2, \dots, 100$) with the one-dimensional chain (red dots) and two-dimensional lattice with 10×5 spins (blue squares). In fig.(3)b we show the dynamical evolution of the fidelity as a func-

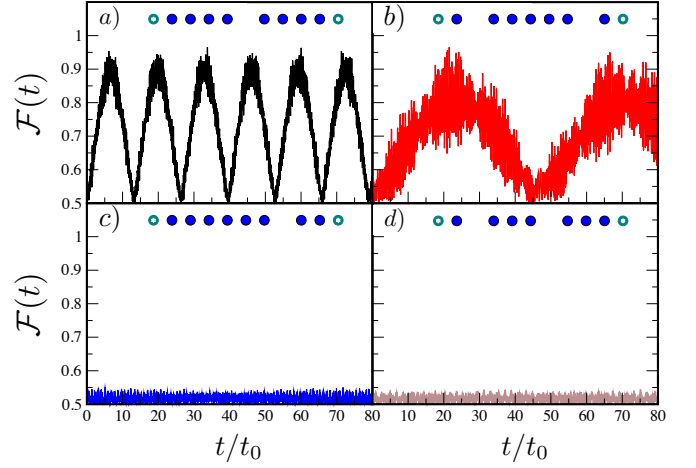


FIG. 4. Quantum state transfer and mirror symmetry of the vacancies in a linear chain with $\alpha = 1$. Dynamical evolution of the fidelity $\mathcal{F}(t)$ with one vacancy a) and c), and two vacancies b) and d). In a)-b) spins are removed symmetrically with respect to the center of the chain. In c)-d) vacancies are created randomly along the chain.

tion of the rescaled time t/t_0 , where we define $t_0 = \pi a^\alpha (N-1)^\alpha / C \hbar^2$. t_0 is the time it takes for the two-spin system (sender and receiver) to perform an ideal quantum state transfer in the absence of the channel. As we discussed in the previous paragraph, a quantitative explanation of the increase of the fidelity can be obtained by studying the eigenstates with maximal overlap with the sender and the receiver. In fig.3c-d we plot the symmetric and antisymmetric eigenstates $\psi_j^{(s,a)}$ which are responsible for the state transfer for the regular chain with N spins (c) and for the two-dimensional lattice 10×5 (d). The effect is an increase of the fidelity and a modification of the period of the oscillations of the fidelity.

The Hamiltonian we consider in our work is mirror symmetric, which in Refs. [8, 10] was found to be a necessary condition for perfect QST. Here we investigate the breaking of the mirror symmetry by removing arbitrary spins in the configurations. For simplicity we focus on one- and two-dimensional systems. The results are reported in fig.(4) and fig.(5).

In fig.(4) we plot the configuration and the dynamics of the QST fidelity in a linear chain with Coulomb interaction $\alpha = 1$ in the presence of one and two vacancies. In a)-b) spins are removed symmetrically with respect to the center of the chain. In c)-d) vacancies are created randomly along the chain. Without mirror symmetry the fidelity decreases to approximately the random guess value of $\frac{1}{2}$. This corresponds to a vanishing probability for the excitation to reach the sender site, see. Eq. 9. However, when in the presence of mirror symmetry, the fidelity has maxima close to 1.

We repeat the analysis for a two-dimensional system with a channel with 9×5 spins. We observe that, preserving mirror symmetry as in fig.(5)a-b, the dynamics

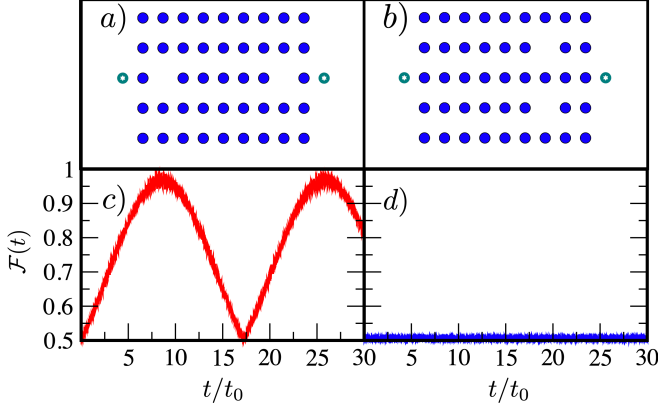


FIG. 5. Quantum state transfer and mirror symmetry of the vacancies in a 2D square lattice with $\alpha = 1$. Dynamical evolution of the fidelity $\mathcal{F}(t)$ with a) two symmetric vacancies and c) two asymmetric vacancies.

displays a high value of the fidelity. In contrast, when mirror symmetry is broken by the removal of two spins, fidelity decreases again to around $\frac{1}{2}$.

B. Finite temperature effects.

We now discuss the effect of disorder in the particle configuration. We focus on the two-dimensional case. However the results can be generalized to both one and three dimensions straightforwardly. The motivation for this analysis is related to recent experiments on Rydberg atoms trapped in optical tweezers. There atoms are trapped in a strongly focussed laser field, with a small but finite dispersion of the position. We model this effect as a temperature-induced quenched disorder on the particle configuration as in [49]. This description is valid if the dynamics of the spin is decoupled from the motional degrees of freedom, i.e. if the time t_{id} associated to the QST protocol is much faster than the typical motional time scales $\hbar/k_B T$, where T is the temperature of the system. Then, we model the dynamics of the motional degrees of freedom of particle i centered in the lattice site with coordinates (x_i^0, y_i^0) with a classical Boltzmann distribution $f(\mathbf{r}, \mathbf{p}) = \exp[-\beta H_m(\mathbf{r}, \mathbf{p})]$, where

$$H_m^{(i)}(\mathbf{r}, \mathbf{p}) = \sum_{j=x,y} \frac{p_j^2}{2m} + \frac{m}{2} \omega_j^2 (r_j - r_j^0)^2. \quad (10)$$

To find the distribution of the position $\bar{f}(x, y)$, we integrate the momentum contribution and normalize

$$\bar{f}(x, y) = \frac{1}{2\pi} \frac{1}{\sigma_x \sigma_y} \exp \left[-\frac{(x - \bar{x})^2}{2\sigma_x^2} - \frac{(y - \bar{y})^2}{2\sigma_y^2} \right], \quad (11)$$

where we defined the variance $\sigma_i^2 = 1/(\beta m \omega_i^2)$. We notice that, although we restrict our analysis to fluctuations

along the plane $x - y$, if we were to fully model an experimental setup, also the confinement along the z direction should be considered. Therefore our study corresponds to the limiting case of vanishing σ_z . For simplicity, we are restricting to $\sigma_x = \sigma_y = \sigma$. We observe that, although particle positions in the lattice are uncorrelated, inter-particle distances (in the definition of the spin exchange couplings J_{ij}) are correlated [50].

The results of the simulations are shown in fig.(6). We plot the distribution of the maxima of the fidelities for gaussian disordered atomic position configurations for several values of the disorder strength σ/a rescaled to the lattice spacing. Particles are displaced with respect to their equilibrium value in a 2D lattice with length $L = 10$ and height $h = 4$. We consider $N_r = 2000$ realizations of the disorder and $\alpha = 1$ Coulomb spin-exchange interaction (a-c) and $\alpha = 6$ van der Waals spin-exchange interaction (d-f). For clarity the distribution is normalized to the peak value of each histogram. Fixing α and for low disorder the distribution is peaked close to unitary fidelities. Increasing the disorder strength a plateau appears in the distribution with a peak at $F_{max} = 1$. By further increasing the disorder the distribution has a peak at $F_{max} = 1/2$ and the plateau disappears. We notice that this behavior is quite generic for the long-range exponents that we analysed. The second relevant feature of the fidelity distributions is that, upon decreasing α smaller values of the disorder σ/a are needed to obtain a distribution peaked at higher fidelities. The qualitative explanation is that a longer-range interaction makes the system more insensitive to the fluctuation of particle positions. To be more quantitative, this can be seen by computing the variation of the spin-exchange couplings as a function of the disorder [51]

$$\frac{\Delta J_{ij}}{J_{ij}} = \frac{\tilde{J}_{ij} - J_{ij}}{J_{ij}} = \frac{r_{ij}^\alpha}{|\mathbf{r}_{ij} + \delta|^\alpha} - 1, \quad (12)$$

where we defined $\mathbf{r}_{ij} = \mathbf{r}_i - \mathbf{r}_j$, $\tilde{J}_{ij} = C/2a^\alpha |\mathbf{r}_{ij} + \delta|^\alpha$, and δ is the difference of the fluctuations of the two particles. Monitoring the variation of $\frac{\Delta J_{ij}}{J_{ij}}$ as a function of α for a fixed equilibrium interparticle spacing and disorder strength, the ratio vanishes for $\alpha = 0$. This corresponds to a position-independent spin coupling that clearly should not depend on the specific value of disorder. In the opposite limit, when α increases the ratio $\frac{\Delta J_{ij}}{J_{ij}}$ decreases to the limiting value -1 for infinite α (position dependent nearest neighbor interaction). In this limit disorder dominates and the regularity of the particle configuration, including a strong breaking of mirror symmetry, leads to a dramatic reduction of the fidelity of the quantum state transfer.

IV. CONCLUSIONS

In this work we studied the problem of quantum state transfer in lattices with open boundary conditions in one,

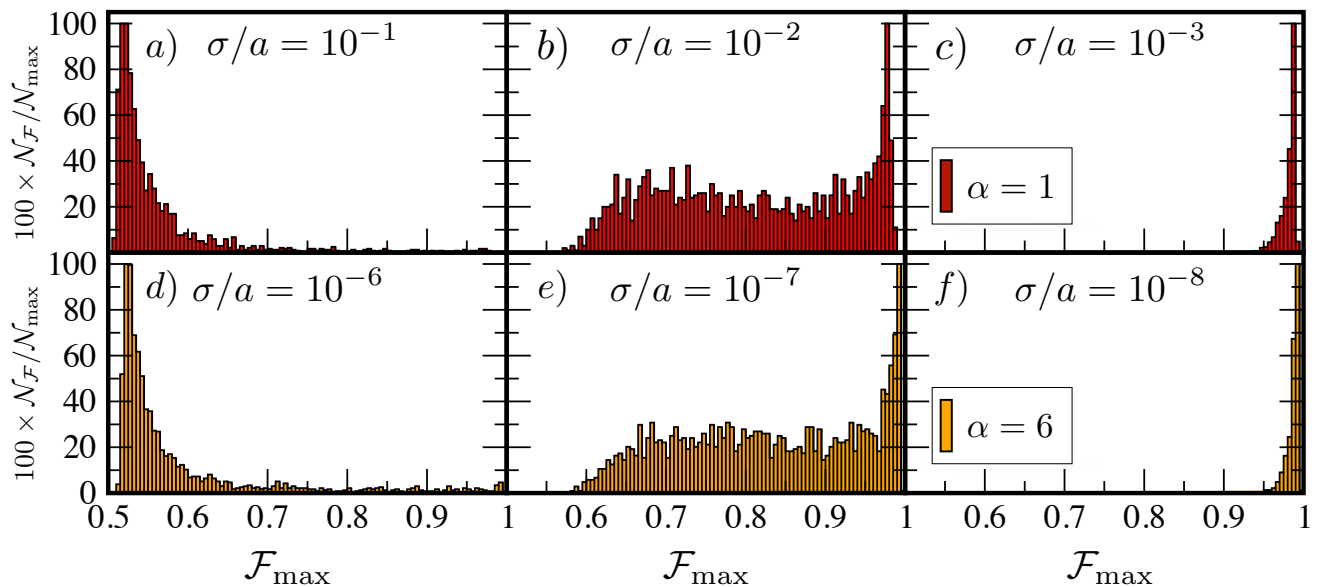


FIG. 6. Distribution of the maxima of the fidelities for gaussian disordered atomic position configurations for several values of the disorder strength. Particles are displaced with respect to their equilibrium value according to a gaussian distribution with width σ/a in a 2D lattice with length $L = 10$ and height $h = 4$. The strength of the disorder is connected to the temperature of the configuration as explained in the text. We consider $N_r = 2000$ realizations. a)-c) $\alpha = 1$ Coulomb spin-exchange interaction. d)-f) $\alpha = 6$ van der Waals spin-exchange interaction. The distribution is normalized to the peak value of each histogram.

two and three dimensions for the anisotropic Heisenberg XXZ model with of power-law couplings with variable exponent α and with a sender and receiver spin symmetrically coupled to its edges.

We first analyzed the case of regular lattices and found that the fidelity increases upon increasing the dimensionality of the lattice for sufficiently large system sizes and the enhancement of the fidelity is more pronounced for systems with long-range interaction. We interpreted this result as a combined effect of the open boundaries of the lattice and the presence of the inter-spin interaction term in the z -direction, resulting in an effective weak-coupling Hamiltonian in the single-excitation sector, although the couplings are all uniform. We justified this interpretation by noticing that the quantum state transfer takes place via Rabi-like oscillations involving only two single-particle eigenstates localized on the sender and receiver site, a mechanism that is related to resonant tunneling in effective decoupled models.

We studied also the effect of vacancies both in one and two dimensional lattices, confirming the necessity of the presence of mirror symmetry in the lattice configuration with the removed spins in order to increase the fidelity of the quantum transfer transfer. Also, for the relevant case of one-dimensional systems, we observed that for longer-range interactions, one might consider a larger number of vacancies to obtain a higher fidelity. Finally, inspired by experiments of cold atoms in optical tweezers, we considered the effect of a finite temperature inducing displacements of the particles by studying the distribution of the maxima of the fidelity. We observed

that, as a general property, longer range interactions suffer less from temperature-induced disorder than shorter range potentials. Quantitatively, this effect can be understood by analyzing the fluctuations of the spin couplings J_{ij} due to disorder as a function of the exponent α .

Our study is relevant for the characterization of quantum state transfer in experimental platforms for quantum simulation and technology. We were mostly inspired by applications to ultracold ions and atoms where long-range interaction are an intrinsic tool in the realization of spin models. Extensions of this work include the study of the effect of decoherence and excited state decay, relevant for experimental platforms. Calculations for open systems will be considered elsewhere.

ACKNOWLEDGMENTS

Acknowledgments. S.H. acknowledges CNPq for financial support. T.M. acknowledges CNPq for support through Bolsa de produtividade em Pesquisa n.311079/2015-6. This work was supported by the Serapilheira Institute (grant number Serra-1812-27802), CAPES-NUFFIC project number 88887.156521/2017-00. T.M. and thanks the Physics Department of the University of L'Aquila for the hospitality where part of the work was done. The authors acknowledge S.M. Giampaolo for useful discussions.

Appendix A: Nearest neighbor interactions in higher lattices

In this Appendix we present the results of the maximum fidelity for nearest neighbor interactions in a slab with linear dimension L and transverse length $L_{\perp} = 5$ in two dimensions and a parallelepiped $L \times L_{\perp} = 5 \times 5$ in three dimensions. For purely one dimensional system, our results are equivalent to [7]. We observe that, similarly to the long-range case, fidelity is higher for a higher dimensional slab. However, the maximum fidelity is notably smaller than unity even for the three-dimensional case, in contrast to Fig.2 where for each $\alpha \leq 6$ fidelity is close to one even for very large sizes.

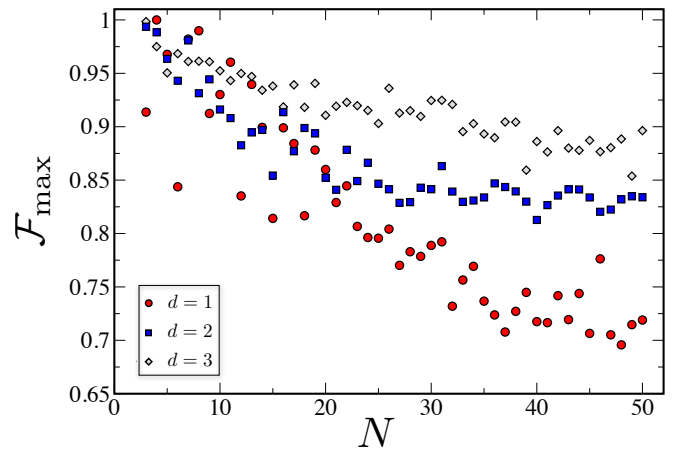


FIG. 7. Maximum fidelity for quantum state transfer in a nearest neighbor interacting system in a one, two and three dimensional slab and $\Delta = 1$ (isotropic Heisenberg model). Red dot: $d = 1$, blue square: $d = 2$, grey diamond: $d = 3$. N is the linear size of the system. In 2D (3D) we consider a square (cubic) lattice with $N \times 5$ ($N \times 5 \times 5$) spins. In 2D the sender and the receiver are located as in Fig.1. In 3D they are located in the center of two opposite faces of the cube, at distance a from the central spin. Fidelity increases with the the dimensionality of the system for sufficiently large system sizes.

-
- [1] T. E. Northup and R. Blatt, Nat Photon **8**, 356 (2014).
 - [2] L.-M. Duan, M. D. Lukin, J. I. Cirac, and P. Zoller, Nature **414**, 413 (2001), arXiv:0105105 [quant-ph].
 - [3] S. Ritter, C. Nölleke, C. Hahn, A. Reiserer, A. Neuzner, M. Uphoff, M. Mücke, E. Figueroa, J. Bochmann, and G. Rempe, Nature **484**, 195 (2012).
 - [4] P. Kurpiers, P. Magnard, T. Walter, B. Royer, M. Pechal, J. Heinsoo, Y. Salathé, A. Akin, S. Storz, J.-C. Besse, S. Gasparinetti, A. Blais, and A. Wallraff, Nature **558**, 264 (2018).
 - [5] C. H. Bennett, G. Brassard, C. Crépeau, R. Jozsa, A. Peres, and W. K. Wootters, Phys. Rev. Lett. **70**, 1895 (1993).
 - [6] X.-S. Ma, T. Herbst, T. Scheidl, D. Wang, S. Kropatschek, W. Naylor, B. Wittmann, A. Meck, J. Kofler, E. Anisimova, V. Makarov, T. Jennewein, R. Ursin, and A. Zeilinger, Nature **489**, 269 (2012).
 - [7] S. Bose, Phys. Rev. Lett. **91**, 207901 (2003).
 - [8] M. Christandl, N. Datta, A. Ekert, and A. Landahl, Physical Review Letters **92**, 1 (2004).
 - [9] D. Burgarth and S. Bose, Phys. Rev. A **71**, 052315 (2005).
 - [10] M. Christandl, N. Datta, T. Dorlas, A. Ekert, A. Kay, and A. Landahl, Physical Review A **71**, 032312 (2005).
 - [11] A. Wójcik, T. Łuczak, P. Kurzyński, A. Grudka, T. Gdala, and M. Bednarska, Physical Review A **72**, 034303 (2005).
 - [12] L. Campos Venuti, C. Degli Esposti Boschi, and M. Roncaglia, Physical Review Letters **99**, 060401 (2007).
 - [13] L. Banchi, T. J. G. Apollaro, a. Cuccoli, R. Vaia, and P. Verrucchi, New Journal of Physics **13**, 123006 (2011).
 - [14] K. Eckert, O. Romero-Isart, and A. Sanpera, New Journal of Physics **9**, 155 (2007).
 - [15] D. Burgarth and S. Bose, New Journal of Physics **7**, 135 (2005).
 - [16] G. M. Almeida, F. A. de Moura, and M. L. Lyra, Physics Letters A **382**, 1335 (2018).
 - [17] T. Osborne and N. Linden, Physical Review A **69**, 1 (2004).
 - [18] C. Di Franco, M. Paternostro, and M. S. Kim, Physical Review Letters **101**, 230502 (2008).
 - [19] C. Di Franco, M. Paternostro, and G. M. Palma, International Journal of Quantum Information **06**, 659 (2008), <https://doi.org/10.1142/S021974990800392X>.
 - [20] S. Paganelli, F. de Pasquale, and G. Giorgi, Physical Review A **74**, 1 (2006).
 - [21] L. Banchi, T. J. G. Apollaro, A. Cuccoli, R. Vaia, and P. Verrucchi, **052321**, 1 (2010).
 - [22] M. B. Plenio and F. L. Semião, New Journal of Physics **7**, 73 (2005), arXiv:0407034 [quant-ph].
 - [23] S. Paganelli, S. Lorenzo, T. J. G. Apollaro, F. Plastina, and G. L. Giorgi, Physical Review A **87**, 062309 (2013).
 - [24] S. Lorenzo, T. J. G. Apollaro, A. Trombettoni, and S. Paganelli, International Journal of Quantum Information **15**, 1750037 (2017).
 - [25] W. J. Chetcuti, C. Sanavio, S. Lorenzo, and T. J. G. Apollaro, “Perturbatively-perfect many-body transfer,” (2019), arXiv:1911.12211 [quant-ph].

- [26] F. Plastina and T. J. G. Apollaro, *Physical Review Letters* **99**, 177210 (2007).
- [27] S. Lorenzo, T. J. G. Apollaro, A. Sindona, and F. Plastina, *Phys. Rev. A* **87**, 42313 (2013).
- [28] F. Mei, G. Chen, L. Tian, S.-L. Zhu, and S. Jia, *Physical Review A* **98**, 012331 (2018), arXiv:1711.07751.
- [29] S. Longhi, G. L. Giorgi, and R. Zambrini, arXiv e-prints, arXiv:1901.05157 (2019), arXiv:1901.05157 [quant-ph].
- [30] S. Bose, *Contemporary Physics* **48**, 13 (2007), arXiv:0802.1224.
- [31] T. J. G. Apollaro, S. Lorenzo, and F. Plastina, *International Journal of Modern Physics B* **27**, 1345035 (2013).
- [32] S. Lorenzo, T. Apollaro, S. Paganelli, G. Palma, and F. Plastina, *Phys. Rev. A* **91**, 42321 (2015).
- [33] R. Sousa and Y. Omar, *New Journal of Physics* **16**, 123003 (2014).
- [34] T. J. G. Apollaro, S. Lorenzo, A. Sindona, S. Paganelli, G. L. Giorgi, and F. Plastina, *Physica Scripta* **T165**, 014036 (2015).
- [35] G. D. de Moraes Neto, F. M. Andrade, V. Montenegro, and S. Bose, *Physical Review A* **93**, 062339 (2016), arXiv:1511.08705.
- [36] U. Farooq, A. Bayat, S. Mancini, and S. Bose, *Physical Review B* **91**, 134303 (2014), arXiv:1411.1270.
- [37] B. E. Kane, *Nature* **393**, 133 (1998).
- [38] D. Loss and D. P. DiVincenzo, *Physical Review A* **57**, 120 (1998).
- [39] F. de Pasquale, G. L. Giorgi, and S. Paganelli, *Physical Review A* **71**, 042304 (2005).
- [40] A. G. Volosniev, D. Petrosyan, M. Valiente, D. V. Fedorov, A. S. Jensen, and N. T. Zinner, *Physical Review A* **91**, 023620 (2015), arXiv:1408.3414.
- [41] R. Vrijen and E. Yablonovitch, *Physica E: Low-dimensional Systems and Nanostructures* **10**, 569 (2001).
- [42] D. Kielpinski, C. Monroe, and D. J. Wineland, *Nature* **417**, 709 (2002).
- [43] M. Saffman, *Journal of Physics B: Atomic, Molecular and Optical Physics* **49** (2016), 10.1088/0953-4075/49/20/202001, arXiv:1605.05207.
- [44] E. H. Lieb and D. W. Robinson, *Commun. math. Phys* **28**, 251 (1972).
- [45] G. Gualdi, V. Kostak, I. Marzoli, and P. Tombesi, *Physical Review A* **78**, 022325 (2008).
- [46] M. Avellino, a. J. Fisher, and S. Bose, *Physical Review A* **74**, 012321 (2006), arXiv:0603148 [quant-ph].
- [47] Z. Eldredge, Z. X. Gong, J. T. Young, A. H. Moosavian, M. Foss-Feig, and A. V. Gorshkov, *Physical Review Letters* **119**, 1 (2017), arXiv:1612.02442.
- [48] N. Y. Yao, L. Jiang, A. V. Gorshkov, Z.-X. Gong, A. Zhai, L.-M. Duan, and M. D. Lukin, *Physical Review Letters* **106**, 040505 (2011).
- [49] D. Barredo, V. Lienhard, S. de Léséleuc, T. Lahaye, and A. Browaeys, *Nature* **561**, 79 (2017), arXiv:1712.02727.
- [50] M. Marcuzzi, J. Miná, D. Barredo, S. de Léséleuc, H. Labuhn, T. Lahaye, A. Browaeys, E. Levi, and I. Lesanovsky, *Physical Review Letters* **118**, 1 (2016), arXiv:1607.06295.
- [51] R. Menu and T. Roscilde, “Anomalous diffusion and localization in a positionally disordered quantum spin array,” (2019), arXiv:1907.12511 [cond-mat.dis-nn].